ARTICLE

Recurrent Mutations in the Basic Domain of *TWIST2* Cause Ablepharon Macrostomia and Barber-Say Syndromes

Shannon Marchegiani,[1,2,31] Taylor Davis,[1,31] Federico Tessadori,[3,31] Gijs van Haaften,[4]
Francesco Brancati,[5] Alexander Hoischen,[6] Haigen Huang,[7] Elise Valkanas,[1] Barbara Pusey,[1]
Denny Schanze,[8] Hanka Venselaar,[6] Anneke T. Vulto-van Silfhout,[6] Lynne A. Wolfe,[1,9]
Cynthia J. Tifft,[1,9] Patricia M. Zerfas,[10] Giovanna Zambruno,[11] Ariana Kariminejad,[12]
Farahnaz Sabbagh-Kermani,[13] Janice Lee,[14] Maria G. Tsokos,[15] Chyi-Chia R. Lee,[15] Victor Ferraz,[16]
Eduarda Morgana da Silva,[16] Cathy A. Stevens,[17] Nathalie Roche,[18] Oliver Bartsch,[19] Peter Farndon,[20]
Eva Bermejo-Sanchez,[21] Brian P. Brooks,[22] Valerie Maduro,[1] Bruno Dallapiccola,[23] Feliciano J. Ramos,[24]
Hon-Yin Brian Chung,[25] Cédric Le Caignec,[26] Fabiana Martins,[27] Witold K. Jacyk,[28] Laura Mazzanti,[29]
Han G. Brunner,[6,30] Jeroen Bakkers,[3] Shuo Lin,[7] May Christine V. Malicdan,[1,9,*] Cornelius F. Boerkoel,[1]
William A. Gahl,[1,9,*] Bert B.A. de Vries,[6] Mieke M. van Haelst,[4] Martin Zenker,[8,32]
and Thomas C. Markello[1,32]

Ablepharon macrostomia syndrome (AMS) and Barber-Say syndrome (BSS) are rare congenital ectodermal dysplasias characterized by similar clinical features. To establish the genetic basis of AMS and BSS, we performed extensive clinical phenotyping, whole exome and candidate gene sequencing, and functional validations. We identified a recurrent de novo mutation in *TWIST2* in seven independent AMS-affected families, as well as another recurrent de novo mutation affecting the same amino acid in ten independent BSS-affected families. Moreover, a genotype-phenotype correlation was observed, because the two syndromes differed based solely upon the nature of the substituting amino acid: a lysine at TWIST2 residue 75 resulted in AMS, whereas a glutamine or alanine yielded BSS. *TWIST2* encodes a basic helix-loop-helix transcription factor that regulates the development of mesenchymal tissues. All identified mutations fell in the basic domain of *TWIST2* and altered the DNA-binding pattern of Flag-TWIST2 in HeLa cells. Comparison of wild-type and mutant *TWIST2* expressed in zebrafish identified abnormal developmental phenotypes and widespread transcriptome changes. Our results suggest that autosomal-dominant *TWIST2* mutations cause AMS or BSS by inducing protean effects on the transcription factor's DNA binding.

Introduction

Ablepharon macrostomia syndrome (AMS [MIM: 200110]) and Barber Say syndrome (BSS [MIM: 209885]) are congenital ectodermal dysplasias.[1–26] AMS is a disorder defined by absent eyelids, macrostomia, microtia, redundant skin, sparse hair, dysmorphic nose and ears, variable abnormalities of the nipples, genitalia, fingers, and hands, largely normal intellectual and motor development, and poor growth (Table 1).[5,6,11,19,20,24] BSS is characterized by

[1]NIH Undiagnosed Diseases Program, Common Fund, Office of the Director, NIH and National Human Genome Research Institute, NIH, Bethesda, MD 20892, USA; [2]Department of Pediatrics, Walter Reed National Military Medical Center, Bethesda, MD 20892, USA; [3]Hubrecht Institute-KNAW and University Medical Centre Utrecht, 3584 CT Utrecht, the Netherlands; [4]Department of Medical Genetics, University Medical Center Utrecht, 3508 AB Utrecht, the Netherlands; [5]Department of Medical, Oral, and Biotechnological Sciences, University of G. d' Annunzio Chieti and Pescara, Chieti 66100, Italy; [6]Department of Human Genetics, Radboud University Medical Center, 6525 GA Nijmegen, the Netherlands; [7]Department of Molecular, Cell, and Developmental Biology, University of California, Los Angeles, Los Angeles, CA 90095, USA; [8]Medizinische Fakultät und Universitätsklinikum Magdeburg, Institute of Human Genetics, 39120 Magdeburg, Germany; [9]Office of the Clinical Director, National Human Genome Research Institute/NIH, Bethesda, MD 20892, USA; [10]Office of Research Services, Division of Veterinary Resources, NIH, Bethesda, MD 20892, USA; [11]Laboratory of Molecular and Cell Biology, Istituto Dermopatico dell'Immacolata IDI-IRCCS, Rome 00167, Italy; [12]Kariminejad-Najmabadi Pathology and Genetics Center, Tehran 14667, Iran; [13]Kerman University of Medical Sciences, Kerman 76175, Iran; [14]National Institute of Dental and Craniofacial Research, NIH, Bethesda, MD 20892, USA; [15]Laboratory of Pathology, National Cancer Institute, NIH, Bethesda, MD 20892, USA; [16]Departamento de Genetica, Faculdade de Medicina de Ribeirao Preto, Universidade de Sao Paulo, Sao Paulo 14049, Brazil; [17]Department of Medical Genetics, T.C. Thompson Children's Hospital, Chattanooga, TN 37403, USA; [18]Department of Plastic and Reconstructive Surgery, University Hospital of Ghent, Ghent 9000, Belgium; [19]Institute of Human Genetics, Johannes Gutenberg University, Mainz 55131, Germany; [20]Clinical Genetics Unit, Birmingham Women's Healthcare Trust, Birmingham B15 2TG, UK; [21]ECEMC (Spanish Collaborative Study of Congenital Malformations), CIAC, Instituto de Investigación de Enfermedades Raras (IIER), Instituto de Salud Carlos III; and CIBER de Enfermedades Raras (CIBERER)-U724, Madrid 28029, Spain; [22]Unit on Pediatric, Developmental, and Genetic Eye Disease, National Eye Institute, NIH, Bethesda, MD 20892, USA; [23]Department of Medical Genetics, Bambino Gesù Children's Hospital, IRCCS, Rome 00165, Italy; [24]Unidad de Genética Médica, Servicio de Pediatría, GCV-CIBERER Hospital Clínico Universitario "Lozano Blesa," Facultad de Medicina, Universidad de Zaragoza, 50009 Zaragoza, Spain; [25]Department of Paediatrics and Adolescent Medicine, Centre for Genomic Sciences, LKS Faculty of Medicine, The University of Hong Kong, Hong Kong SAR, China; [26]Service de genetique medicale, CHU Nantes, 44093 Nantes, France and Inserm, UMR957, Faculté de Médecine, 44093 Nantes, France; [27]Special Care Dentistry Center, Department of Stomatology, School of Dentistry, University of São Paulo, São Paulo 05508-070, Brazil; [28]Department of Dermatology, University of Pretoria, Pretoria 0028, Republic of South Africa; [29]Department of Pediatrics, S. Orsola-Malpighi Hospital University of Bologna, 40138 Bologna, Italy; [30]Department of Clinical Genetics, Maastricht University Medical Center, PO Box 5800, 6202AZ Maastricht, the Netherlands
[31]These authors contributed equally to this work
[32]These authors contributed equally to this work and are co-senior authors
*Correspondence: malicdanm@mail.nih.gov (M.C.V.M.), gahlw@helix.nih.gov (W.A.G.)

Table 1. Clinical Features of Individuals Harboring *TWIST2* Mutations

Subject	TWIST2 Alteration	Gender	Eyelids	Mouth	Nose	Ears	Skin	Hair	Nipples	Genitalia	Hands	Other	Development
AMS-1.1[20]	p.Glu75Lys	M	severe hypoplastic eyelids bilateral	macrostomia	depressed nasal bridge	microtia first degree, cryptotia, low-set	wrinkled	sparse	normal	ambiguous	normal	hypertelorism	normal
AMS-2.1[9]	p.Glu75Lys mosaic	M	right upper eyelid defect, absent eyelashes	normal	normal	microtia first degree, increased posterior angulation	normal	sparse	normal	normal	normal	–	normal
AMS-2.2[9]	p.Glu75Lys paternally inherited	F	ablepharon bilateral	macrostomia	depressed nasal bridge, under-developed ala ansi	microtia first degree, low-set	redundant	sparse, absent lanugo	hypoplastic	hypoplastic labia majora	cutaneous syndactyly	hypertelorism	–
AMS-2.3[9]	p.Glu75Lys paternally inherited	F	ablepharon bilateral	macrostomia	depressed nasal bridge, anteverted nostrils	microtia first degree	thin, redundant	sparse, absent lanugo	absent	hypoplastic labia majora	small nails	omphalocele, anteriorly placed anus	–
AMS-3.1 (case 2 in Stevens and Sargent[24])	p.Glu75Lys de novo	M	ablepharon bilateral	macrostomia	depressed nasal bridge, cleft ala nasi	microtia first degree, low-set	thin, wrinkled	sparse, absent lanugo	hypoplastic	ambiguous genitalia, micropenis, cryptorchidsim	cutaneous syndactyly, camptodactyly	single umbilical artery, lipoma overlying metopic suture	mild gross and fine motor delay, articulation errors with speech
AMS-4.1 (case 3 in Stevens and Sargent[24])	p.Glu75Lys de novo	F	ablepharon bilateral	macrostomia	depressed nasal bridge, cleft ala nasi	microtia first degree, low-set, unilateral hearing loss	thin, wrinkled	sparse, absent lanugo	normal	hypoplastic labia majora, urethral opening in vagina	camptodactyly	hemiparesis due to cerebral hemorrhage, anteriorly placed anus	mild delays, receives PT, OT, and speech therapy
AMS-5.1 (case 4 in Stevens and Sargent[24])	p.Glu75Lys de novo	F	ablepharon bilateral	macrostomia	cleft ali nasi	microtia first degree, mild hearing loss	thin, wrinkled	sparse, absent lanugo	hypoplastic	normal	camptodactyly	zygomatic hypoplasia	normal
AMS-6.1[5]	p.Glu75Lys mosaic	F	severe hypoplastic eyelids bilateral, absent eyelashes	macrostomia	under-developed ala nasi	microtia first degree, high-frequency hearing loss	thin, wrinkled	sparse	hypoplastic nipples and breast	normal	cutaneous syndactyly, camptodactyly	aplastic zygomatic arches	normal
AMS-7.1[22]	p.Glu75Lys mosaic	M	severe hypoplastic eyelids bilateral	macrostomia?	normal	microtia first degree	redundant	variable follicle density on posterior scalp	normal	ambiguous genitalia	clinodactyly radial f5 bilateral	low anterior hairline, omphalocele	normal

(*Continued on next page*)

Table 1. *Continued*

Subject	TWIST2 Alteration	Gender	Eyelids	Mouth	Nose	Ears	Skin	Hair	Nipples	Genitalia	Hands	Other	Development
AMS-7.2[22]	p.Glu75Lys paternally inherited	M	ablepharon bilateral	macrostomia	under-developed ala nasi	microtia first degree	thin, redundant	sparse, absent lanugo	normal	hypoplasia of labia majora	cutaneous syndactyly	omphalocele, anteriorly placed anus, absent zygomatic arches	mild gross motor delay, mild receptive language delay, significant early expressive language delay
BSS-1.1[10]	Gln77_Arg78dup de novo	F	severe hypoplastic eyelids bilateral, ectropion	macrostomia	bulbous nose	cup-shaped, hypoplastic external auditory canals, hearing loss	wrinkled, dry	marked hypertrichosis	inverted	"snout-shaped" labia majora	normal	velopharyngeal incompetence	delayed language development, dyslalia, dysgrammatism
BSS-2.1[14]	p.Glu75Gln de novo	F	ectropion	macrostomia	broad nasal width, bulbous nose, hypoplastic ala nasi	microtia first degree, hypoplastic external auditory canals	wrinkled, translucent	marked hypertrichosis	normal	ambiguous	normal	parental consanguinity	–
BSS-3.1 (this paper)	p.Glu75Gln de novo	F	ectropion	macrostomia	broad nasal width, bulbous and prominent nose	small, hypoplastic external auditory canals	wrinkled, visible veins over thorax	marked hypertrichosis	hypoplastic	normal	normal	low anterior hairline, sparse eyebrows, hypertelorism, hypoplastic maxilla, gum hypertrophy, widely spaced teeth	mild delay
BSS-4.1[21]	p.Glu75Gln mosaic	M	coarse eyebrows, telecanthus	macrostomia	bulbous nose, broad nasal width	normal	redundant, dry skin	marked hypertrichosis	inverted, hypoplastic	normal	normal	low anterior hair line	normal
BSS-4.2[21]	p.Glu75Gln paternally inherited	F	ectropion, telecanthus, epiblepharon	macrostomia, mild micrognathia	bulbous nose, broad nasal width	low-set ears, small external canal, concha, extra fold	redundant, dry skin, lipodystrophy	marked hypertrichosis	inverted, hypoplastic	normal	normal	low anterior hair line, thin vermillion of lips	normal
BSS-4.3[21]	p.Glu75Gln paternally inherited	F	ectropion, ocular telecanthus, epiblepharon	macrostomia, mild micrognathia	bulbous nose, broad nasal width	low-set ears, microtia first degree, concha extra fold	redundant, dry skin, lipodystrophy	marked hypertrichosis	inverted, hypoplastic	normal	normal	low anterior hair line, thin vermillion of lips	normal
BSS-5.1[25]	p.Glu75Gln	M	ectropion bilateral, sparse lashes	macrostomia	bulbous nose	microtia first degree	lax, redundant skin	marked hypertrichosis	hypoplastic	shawl scrotum	normal	clubfeet, reduced elastic fibers on skin biopsy	–
BSS-6.1 (this paper)	p.Glu75Ala de novo	F	hypoplasia, microblepharon, ectropion (bilateral)	macrostomia	broad nasal width, bulbous nose, hypoplastic ala nasi	microtia first degree	thin (general), redundant (trunk)	marked hypertrichosis (back and limbs)	hypoplastic	mild hypoplasia of labia majora	brachydactyly and clinodactyly f5 prominent digit pads	high palate, lumbar flat angioma	normal

Table 1. Continued

Subject	TWIST2 Alteration	Gender	Eyelids	Mouth	Nose	Ears	Skin	Hair	Nipples	Genitalia	Hands	Other	Development
BSS-7.1[15]	p.Glu75Gln de novo	F	microblepharon, ectropion	macrostomia	broad nasal width, bulbous nose	microtia first degree, low-set	thin, redundant	marked hypertrichosis, lanugo hair, sparse eyebrows	absent	normal	normal	parental consanguinity, telengectasias, hypdontia malocclusion	normal
BSS-8.1[7]	p.Glu75Gln	M	ectropion bilateral	macrostomia	bulbous nose, anteverted nares	microtia first degree, hypoplasia external auditory canals	redundant	marked hypertrichosis	hypoplastic	bilateral cryptorchidism	normal	hypertelorism	normal
BSS-9.1 (this paper)	p.Glu75Gln de novo	F	ectropion/ bilateral "lagophthalmos" as described by ophthalmologist	macrostomia	bulbous nose	microtia first degree	thin, wrinkled	marked hypertrichosis over the back	hypoplastic	normal	normal	hypertelorism	normal
BSS-10.1[16]	p.Glu75Ala	F	ectropion bilateral, sparse lashes	macrostomia	bulbous nose, broad nasal width	microtia first degree, narrow auditory canal	lax, redundant skin	marked hypertrichosis	hypoplastic	hypoplastic labia minora	normal	hypertelorism, delayed eruption of teeth	mild language delay

Shown are the clinical features of individuals with ablepharon macrostomia syndrome (AMS) and Barber Say syndrome (BSS) and mutation included in this study. Description of signs and symptoms adhere to the published guidelines according to the Elements for Morphology recommendations.[27–34] Mutations in TWIST2 (GenBank: NM_057179.2) account for all cases in the study.

ectropion, macrostomia, ear abnormalities, bulbous nose with hypoplastic alae nasi, redundant skin, hypertrichosis, and variable other features.[14,16,21,23,25,26] Several instances of parent-to-child transmission suggest that both AMS and BSS are inherited in an autosomal-dominant fashion,[2,8,9,21,22] but no specific gene defect has been associated with these disorders. The substantial phenotypic overlap between AMS and BSS, as well as a shared mode of inheritance, supports the hypothesis that the two disorders are caused by dominant mutations in the same gene.[10,15,16]

We employed extensive clinical phenotyping, exome sequencing, and expression studies to determine the genetic basis for AMS and BSS. We show that both AMS and BSS are due to dominant mutations in TWIST2 (MIM: 607556), affecting a highly conserved residue. TWIST2 (also called Dermo-1), which binds to E-box DNA motifs (5′-CANNTG-3′) as a heterodimer with other bHLH proteins such as the ubiquitously expressed protein E12, is thought to act as a negative regulator of transcription.[35–40] TWIST2 expression is temporally restricted and tissue specific. During embryonic development, TWIST2 is highly expressed in the craniofacial mesenchyme and in chondrogenic precursors. Previous studies suggest that TWIST2 regulates mesenchymal stem cell differentiation and directs the development of dermal and chondrogenic tissues.[35,38,40,41] Disturbance of these processes due to dominant mutations in TWIST2 could, therefore, cause the distinctive clinical features and facial patterning defects observed in AMS and BSS. Molecular analyses suggest that these mutations alter the DNA-binding activity of TWIST2, leading to both dominant-negative and gain-of-function effects.

Methods

Individuals Included in the Study

The original six family members of a pedigree including AMS-7.1 and AMS-7.2 were enrolled in the NIH Undiagnosed Diseases Program and admitted to the National Institutes of Health Clinical Center (NIH-CC). That family, together with AMS-6.1, were enrolled in protocol 76-HG-0238, "Diagnosis and Treatment of Patients with Inborn Errors of Metabolism or Other Genetic Disorders," approved by the National Human Genome Research Institute (NHGRI) Institutional Review Board (IRB). Targeted genetic testing, karyotype analysis, and chromosomal microarray analysis revealed no significant findings. SNP array analysis showed no anomalous regions of homozygosity or significant copy-number variants. Studies of 7 additional AMS-affected individuals from 5 families and 12 BBS-affected individuals from 10 families were approved by the institutional review boards of the Policlinico Tor Vergata University Hospital, the University of Magdeburg, University Medical Center Utrecht, Ghent University Hospital, and Radboud University Medical Center Nijmegen. Written informed consent was obtained from all affected individuals or parents.

Electron Microscopy

Skin biopsies were fixed for 48 hr at 4°C in 2% glutaraldehyde in 0.1 M cacodylate buffer (pH 7.4) and washed with cacodylate

buffer three times. The tissues were fixed with 2% OsO$_4$ for 2 hr, washed again with 0.1 M cacodylate buffer three times, washed with water, and placed in 1% uranyl acetate for 1 hr. The tissues were subsequently serially dehydrated in ethanol and embedded in Spurr's (Electron Microscopy Sciences). Semi-thick (~1,000 nm) and thin (~80 nm) sections were obtained by utilizing the Leica ultracut-UCT ultramicrotome (Leica) and placed either on glass slides for toluidine blue staining or onto 300 mesh copper grids and stained with saturated uranyl acetate in 50% methanol and then with lead citrate. The grids were viewed in the JEM-1200EXII electron microscope (JEOL Ltd) at 80 kV and images were recorded on the XR611M, mid mounted, 10.5 Mpixel, CCD camera (Advanced Microscopy Techniques).

Fibroblast Culture
Primary dermal fibroblasts were cultured from forearm skin-punch biopsies as described.[42] Genomic DNA was extracted from AMS-3.1, -6.1, -7.1 (hyperpigmented, affected), and -7.2 and from BSS-4.2 and -6.1 dermal fibroblasts as well as ATCC adult control, AMS-7.1 (hypopigmented, unaffected), and the mother of AMS-7.2 dermal fibroblasts as unaffected control.

Genetic Analysis
Genomic DNA was extracted from whole blood of AMS-7.1 and AMS-7.2 and their unaffected family members via the Gentra Puregene Blood Kit (QIAGEN). SNP analyses were performed with an Illumina Omni Express 12 (hg18) SNP array and the Genome Studio software program. Whole-exome sequencing was performed with the Illumina HiSeq2000 platform and the TrueSeq capture kit (Illumina) by the NIH Intramural Sequencing Center (NISC). Sequence data were aligned to the human reference genome (hg19) via Novoalign (Novocraft Technologies). Variants were filtered based on allele frequencies in the NIH Undiagnosed Diseases Program[43–45] cohort (<0.06) and were confirmed by Sanger sequencing.

Protein Modeling
A computerized model of TWIST2 bound to DNA was generated by YASARa and WHAT IF Twinset via standard parameters with PDB: 1NKP (Myc-Max Recognizing DNA) as template. A homodimeric model was produced by superimposing two TWIST2 models on the original PDB: 1NKP file.

ChIP-Seq
Stably transfected T-REx-HeLa cells, treated for 24 hr with 1 μg/ml tetracycline to induce recombinant WT, p.Glu75Lys, p.Glu75Gln, p.Glu75Ala, and p.Gln77_Arg78dup TWIST2 overexpression, were fixed, pelleted, and frozen according to a cell fixation protocol provided by Active Motif. Sheared chromatin from T-REx HeLa cells without recombinant TWIST2 served as a negative control and was similarly fixed, pelleted, and frozen as a negative control. Chromatin shearing, ChIP, and DNA sequencing were performed by Active Motif. ChIP was performed with a monoclonal anti-FLAG M2 antibody (Sigma Aldrich). ChIPed DNA was sequenced on the Illumina NextSeq 500 platform. Short reads were aligned to human reference genome (hg19) with BWA.[46] Binding peaks were identified with MACS using standard parameters.[47] Peaks shared between different samples as well as the Jaccard coefficients representing the correlations between samples were calculated with BedTools.[48] Peaks were annotated and summarized with CEAS.[49] The consensus-binding motif for the WT TWIST2 sample

peaks was determined with GEM2.5 with a minimum k-mer length of 6 and a maximum k-mer length of 20.[50]

Plasmids and Transfection
pCMV6 plasmid containing human TWIST2 cDNA was purchased from Origene Technologies. TWIST2 cDNA was amplified by PCR with Platinum Taq DNA Polymerase High Fidelity (Life Technologies) using pCMV6/TWIST2 plasmid as template. PCR amplification was performed with a forward primer containing FLAG-HA tags. The PCR product was then cloned into the Gateway entry vector pENTR/D-TOPO (Life Technologies) according to the manufacturer's protocol. Mutations associated with AMS and BSS (c.223G>A [p.Glu75Lys], c.223G>C [p.Glu75Gln], c.224A>C [p.Glu75Ala], and c.229_234dupCAGCGC [p.Gln77_Arg78dup]) were introduced into the TWIST2 containing pENTR/D-TOPO plasmid with the QuikChange Lightning Site-Directed Mutagenesis kit (Agilent) according to manufacturer's protocol. All primer sequences are listed in Table S1. TWIST2 inserts were then recombined into the Gateway mammalian expression plasmid pT-REx-DEST30 (Life Technologies) according to the manufacturer's protocol.

T-REx-HeLa cells (Life Technologies) were grown in Dulbecco's Modified Eagle's Medium (DMEM) containing 10% (v/v) heat-inactivated fetal bovine serum, 1% (v/v) penicillin-streptomycin, and 5 μg/ml blasticidin. T-REx-HeLa cells were transfected with 2.5 μg pT-REx-DEST30 vector with Lipofectamine 2000 reagent (Life Technologies) and selected with 400 μg/ml Geneticin. Individual clones were screened for TWIST2 expression before and after 24 hr treatment with 1 μg/ml tetracycline. Clones with the highest expression after 24 hr and with minimal leaky expression were chosen for use in further assays.

Zebrafish Experiments
Zebrafish (*Danio rerio*) were maintained under an approved animal study protocol, in accordance with the Zebrafish Book.[51] The human wild-type and mutant *TWIST2* (p.Glu75Lys and p.Glu75Gln) were cloned into pCS2GW by Gateway (Life Technologies). Subcloned cDNAs were linearized and used for in vitro synthesis of capped mRNA via mMESSAGE mMACHINE SP6 Ultra Kit (Life Technologies). Wild-type embryos of Tupfel long fin (TL) strain embryos were injected at the one-cell stage with 10 pg (phenotypical analysis) or 2 pg (RNA sequencing) mRNA. Embryos were raised at 28°C in Embryo Medium (E3).

For RNA sequencing, total RNA was extracted from approximately 70 non-injected, wild-type h*TWIST2* mRNA-injected, p.Glu75Lys mRNA-injected, and p.Glu75Gln mRNA-injected zebrafish embryos at shield stage in triplicate. Each embryo was microinjected with approximately 10 pg mRNA. RNA extraction was carried out with TRizol (Life Technologies BV) according to the manufacturer's recommendations. For all samples, total RNA was re-suspended in MQ water prior to sequencing. RNA-seq libraries were prepared according the TruSeq Stranded Total RNA Sample Preparation, Low Sample (LS) protocol. The 12 RNA-seq samples were run on a single HiSeq2500 flow cell. Quality control in FastQ files was performed with FastQC, followed by alignment to the zebrafish genome via STAR.[52] A second-quality control step was performed on the generated BAM files via Picards collectRNAMetrics. The read count per gene was determined by HTSeq-count and normalized with DESeq.[53] Differential expression analysis was done on the normalized read count tables. GO term analysis was carried out with Gorilla in fast mode[54,55]

Figure 1. Clinical, Histological, and Molecular Defects in Ablepharon-Macrostomia Syndrome and Barber-Say Syndrome

(A) Face, shoulders, and hands of AMS-6.1, AMS-7.1, and AMS-7.2, demonstrating dysmorphic features detailed in Table 1. Shoulder photographs of AMS-6.1 and AMS-7.1 highlight Blaschko-like hyperpigmented banding indicative of mosaicism. Hands show mild cutaneous syndactyly and clinodactyly.

(B) Electron microscopy of skin of unaffected control (1), AMS-6.1 (2), AMS-7.1 (3), and AMS-7.2. In (1), the elastin (asterisk) is ovoid in shape, whereas in (2), (3), and (4), the elastin appears elongated and, in some areas, fractured. Collagen fibers in (1) appear organized and are oriented in bundles. In (3) and (4), some collagen fibers appear in disarray (arrows) and show curved edges. In addition, some collagen fibers show variable diameters (6). Surrounding the elastin in (5) (AMS-7.1) and (6) (AMS-7.2) are flocculent and amorphous deposits that disrupt organization of collagen bundles. Scale bars represent 1,000 nm (1–4) and 500 nm (5 and 6).

(C) Face, back, and hands of BSS-3.1 and BSS-4.2 showing dysmorphic features detailed in Table 1. Note hypertrichosis.

(D) Electron microscopy of skin of BSS-3.1. Note the long and thin elastin fibers (asterisk) and collagen fibers in disarray (arrow) in (1). Similar to AMS, some collagen fibers show variable diameters (2). Surrounding the elastin in (3) are flocculent and amorphous deposits that disrupt organization of elastin and collagen bundles. Scale bars represent 1,000 nm (1) and 500 nm (2 and 3).

on the expression profiles of the top 10,000 protein-coding genes ranked on adjusted p value from zebrafish embryos overexpressing h*TWIST2* variants. The analysis was carried out on datasets of 26,457 protein-coding genes for p.Glu75Lys and p.Glu75Gln after comparison with wild-type h*TWIST2*-overexpressing samples.

Results

Clinical Characteristics

The clinical features of the AMS-affected cohort were previously described in the literature, and their findings and the original citations are listed in Table 1. Overall, the persons with AMS exhibited ablepharon or microblepharon, macrostomia, varying anomalies of the nose and ears, lax redundant skin, sparse hair, variable abnormalities of the nipples, genitalia, fingers, and hands, and largely normal intellectual and motor development. AMS-6.1, AMS-7.1, and AMS-7.2 have typical facial, extremity, and adipose features typical of AMS (Figure 1A). Extensive craniofacial phenotyping of AMS-7.2 also identified undescribed features of harlequin-shaped eyebrows with absence of the distal third, a hypoplastic nasal dorsum with no projection of the nasal tip, absent columella, hypoplastic ala nasi, macrostomia, CL II malocclusion with 50% overbite, a Brody bite, conical shaped teeth, and a long uvula. The macrostomia was characterized by deficient lateral devel-

opment of the vermillion border and an inability to raise the oral commissures upon smiling, suggesting a discontinuity of the orbicularis oris muscle. Electron microscopy of skin biopsies of AMS-7.1 and AMS-7.2 showed thin, disrupted elastic fibers with areas of amorphous deposits along abnormally oriented collagen fibers and adjacent areas of microfibrillar proliferation (Figure 1B). Masson-Trichrome staining showed abnormal reticulodermal collagen patterns in AMS-7.1 and AMS-7.2 (Figure S1A), whereas elastic fiber (Elastic Van Geison) staining appeared within normal limits (Figure S1B).

The BSS-affected individuals exhibited ectropion, macrostomia, bulbous noses, malformed ears in the spectrum of microtia first degree, thin, redundant skin, hypertrichosis, hypoplastic nipples, and normal hands and development, together with other variable features (Table 1; Figure 1C). Electron microscopy of the skin biopsy of BSS-3.1 showed findings similar to those of AMS, i.e., thin and long elastic fibers, abnormally oriented collagen fibers, and areas of microfibrillar proliferation and amorphous deposits (Figure 1D). BSS-3.1 and BSS-9.1 have not been previously reported; their clinical features are detailed in Table 1.

DNA Studies

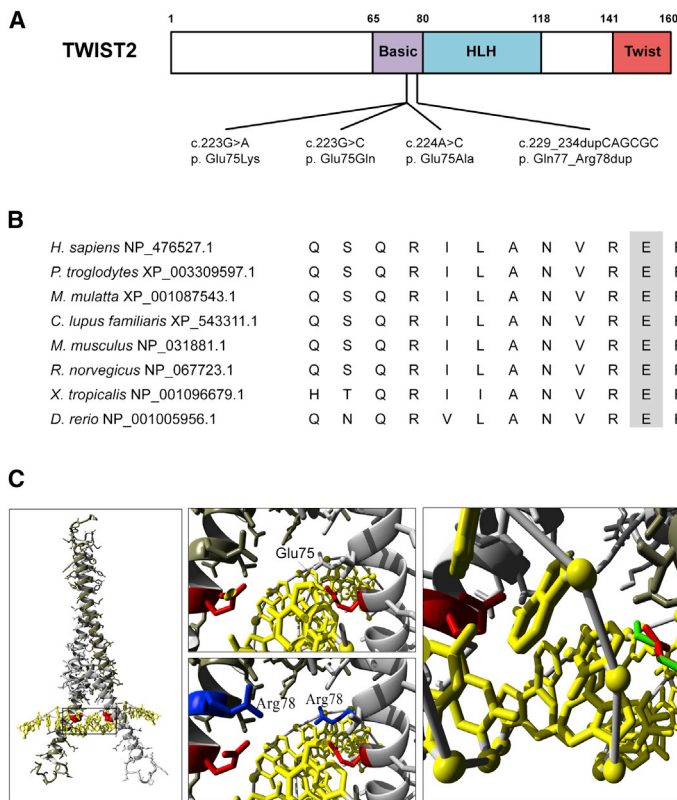Initial studies were performed on two individuals with AMS (7.1 and 7.2), members of a three-generation

Figure 2. Mutations in the Basic Domain of TWIST2 Associated with AMS and BSS
(A) Schematic of *TWIST2* (GenBank: NP_476527.1) with locations of de novo missense variants identified in individuals with AMS and BSS.
(B) Protein sequence alignment of vertebrate TWIST2 homologs. Residues in the basic domain affected by de novo variants are shaded gray.
(C) Dimeric TWIST2 bHLH protein (gray) with bound DNA (yellow) model with inset. The p.Glu75 residue (red) is oriented toward the DNA major grove; this residue could be involved in hydrogen bonding with the first two nucleotides of the consensus E-box motif or positioning residue p.Arg78.

databases such as NHGRI CLINSEQ,[36] dbSNP 142,[35] 1000 Genomes Project Database, NHLBI Exome Sequencing Project EVS v.0.0.30, or the ExAC database (see Web Resources).

Protein Modeling
TWIST2 contains three functional domains: basic, helix-loop-helix, and twist box (Figure 2A). The *TWIST2* alterations associated with AMS and BSS (p.Glu75Lys, p.Glu75Gln, p.Glu75Ala, and p.Gln77_Arg78dup) all fall within the basic domain of the protein, which mediates DNA binding. The residues affected in AMS and BSS are conserved from zebrafish to human (Figure 2B). In silico TWIST2 modeling suggests that mutations affecting the p.Glu75 residue do not alter global protein structure but could alter DNA binding (Figure 2C). The p.Glu75 residue is putatively oriented toward the major groove of bound DNA and in close proximity to the first two nucleotides of the E-box motif. Therefore, the mutations associated with AMS and BSS (as well as p.Gln77_Arg78dup) could alter the DNA-binding activity of TWIST2.

pedigree. Targeted genetic testing, karyotype analysis, and chromosomal microarray analysis revealed no significant findings. SNP array analysis showed no anomalous regions of homozygosity or significant copy-number variants. Exome sequencing on all family members revealed a single nonsynonymous heterozygous mutation in *TWIST2*, c.223G>A (GenBank: NM_057179.2), encoding the predicted deleterious protein alteration p.Glu75Lys. Targeted sequencing revealed the same *TWIST2* mutation in ten AMS-affected individuals from seven independent families (Table 1). Targeted sequencing of 11 BSS-affected individuals (Figure 1B) identified heterozygous missense mutations; nine had a c.223G>C (p.Glu75Gln) mutation (GenBank: NM_057179.2) and two had c.224A>C (p.Glu75Ala) mutations (GenBank: NM_057179.2). A 12th individual with BSS, BSS-1.1, carried a heterozygous c.229_234dupCAGCGC (p.Gln77_Arg78dup) mutation (GenBank: NM_057179.2) in *TWIST2* (Table 1).

In all instances in which DNA was available from both unaffected parents, the *TWIST2* mutation occurred de novo in the first generation of individuals affected with AMS or BSS and was heritable in the third generation. Three disease-transmitting fathers with mild AMS or BSS and variable skin pigmentation were mosaic for a *TWIST2* mutation, based upon next-generation sequencing of peripheral blood DNA (AMS-6.1) and Sanger sequencing of DNA from affected and unaffected skin (AMS-7.1) (Figure S2). None of the disease-causing *TWIST2* mutations were present in the NIH Undiagnosed Diseases Program's exome cohort, and none were reported in public variant

Wild-Type and Mutant TWIST2 Binding Sites
We characterized the binding pattern of both wild-type and mutant TWIST2 in an agnostic and genome-wide fashion. Specifically, we performed ChIP-seq on sheared cross-linked chromatin from T-REx HeLa cells overexpressing recombinant FLAG-HA-tagged TWIST2 proteins; sheared chromatin from T-REx HeLa cells without recombinant TWIST2 served as a negative control. We identified 630 binding peaks associated with wild-type TWIST2. Events associated with wild-type TWIST2 binding were significantly enriched (p < 0.05) near promoters (<1,000 bp, <2,000 bp, and <3,000 bp) as well as in 5' UTRs (data not shown). The consensus binding motif determined for wild-type TWIST2 was 5'-CATCTGG-3' (Figure 3A), which represents a canonical E-box. The
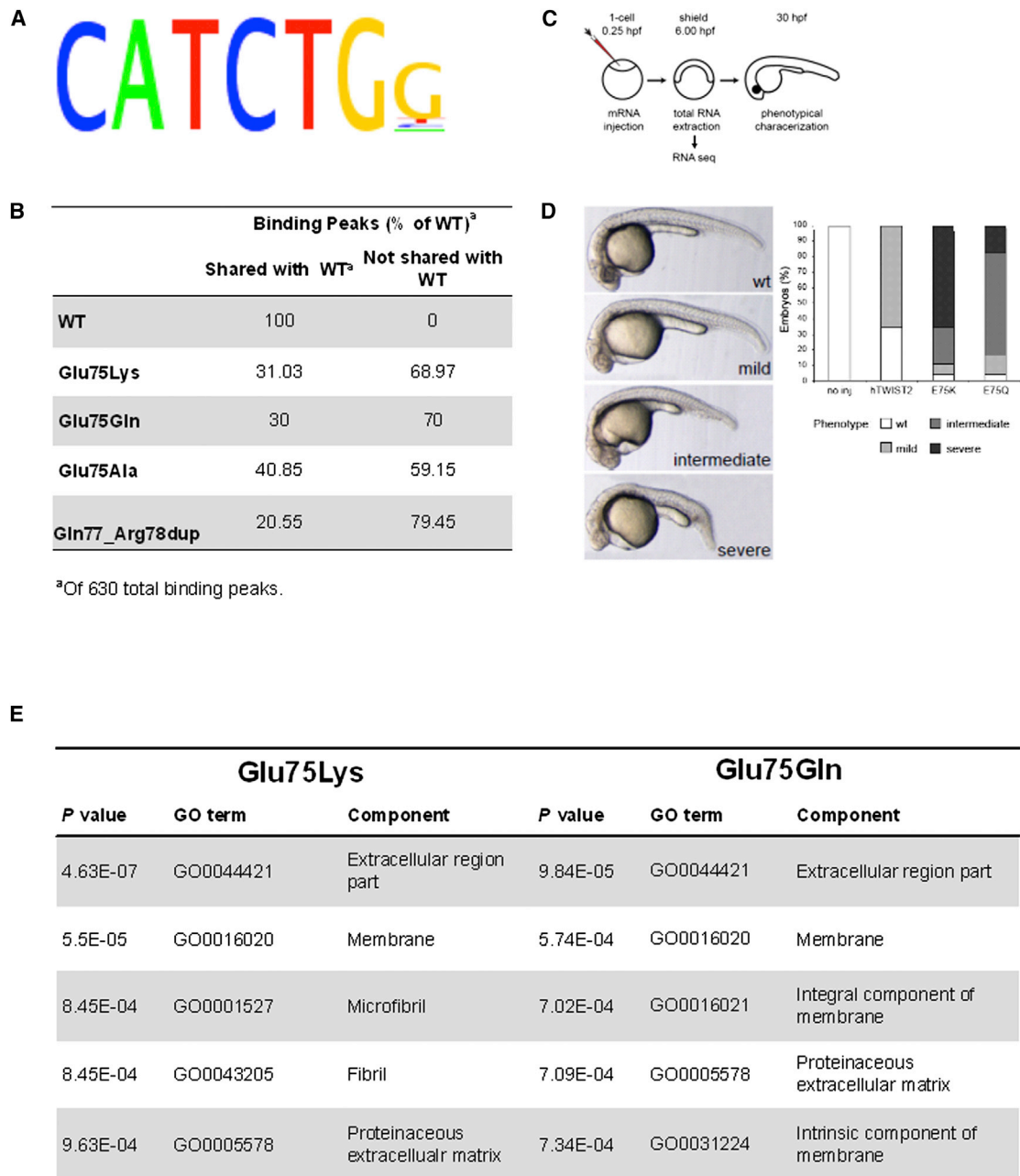
Figure 3. Effect of TWIST2 Mutations on HeLa Cell DNA Binding Sites and on Zebrafish Development and Gene Expression

(A) Chromatin from HeLa cells overexpressing wild-type TWIST2 was subjected to ChIP-seq, identifying 630 DNA binding sites with a consensus sequence typical of an E-box motif.

(B) ChIP-seq showed that the numbers of binding sites for p.Glu75Lys, p.Glu75Gln, p.Glu75Ala, and p.Gln77_Arg78dup TWIST2 were reduced compared to WT TWIST2 and that the mutants bound to many sites not shared with WT TWIST2.

(C) Schematic of the zebrafish studies, involving embryos microinjected with mRNA at the 1-cell stage and either used at shield stage (6 hpf) for RNA-seq or left to grow until approximately 30 hpf for phenotypic characterization.

(D) Appearance of mild, moderate, and severely affected embryos, and quantification of the phenotypes induced at 30 hpf by overexpression of WT, p.Glu75Lys, and p.Glu75Gln hTWIST2. Embryos were injected at the 1-cell stage with 10 pg mRNA. hTWIST2 variants induced defects in head structures and failure of the posterior end of the embryo to extend properly. The p.Glu75Lys and p.Glu75Gln mutants induced stronger developmental defects than wild-type hTWIST2 mRNA.

(E) GO term analysis on ranked gene lists from RNA-seq for p.Glu75Lys and p.Glu75Gln mRNA. Extracellular matrix, membrane, and cytoskeleton proteins are downregulated.

TWIST2 alterations (p.Glu75Lys, p.Glu75Gln, p.Glu75Ala, and p.Gln77_Arg78dup) shared only a fraction of their binding peaks with WT TWIST2 (Figure 3B); p.Glu75Ala and p.Gln77_Arg78dup TWIST2, both associated with BSS, shared only 25 binding peaks in common with the wild-type. A significant number of binding peaks detected for the mutant TWIST2 proteins were not detected for the wild-type protein (Figure 3B).

TWIST2 and Zebrafish Development

To elucidate the effect of *TWIST2* mutations in vivo, we assessed the functional consequences of injecting wild-type and mutant (p.Glu75Lys and p.Glu75Gln) human *TWIST2* (*hTWIST2*) mRNA into zebrafish at the 1-cell stage (Figure 3C). The introduction of wild-type *hTWIST2* led to mild developmental defects (mainly mild brain hypoplasia) in approximately 65% of injected zebrafish (Figure 3D). The injection of p.Glu75Lys and p.Glu75Gln *hTWIST2* RNA, however, led to predominantly intermediate and severe developmental defects, including severe head hypoplasia, unclear midbrain-hindbrain boundary, dysmorphic body trunk, and pericardial edema. These results were confirmed in stable transgenic zebrafish lines that express human wild-type and mutant *TWIST2* (p.Glu75Lys and p.Glu75Gln) under the control of a Cre-loxP inducible system (Figure S3A).

To gain insight into the genetic processes underlying the developmental phenotypes, we performed RNA sequencing on injected embryos at shield stage. Compared to injection of wild-type *hTWIST2*, injection of p.Glu75Lys or p.Glu75Gln *hTWIST2* caused differential expression of 162 genes from a total of 26,457 datasets (adjusted p value < 0.05); of these, 28 were common to both p.Glu75Lys and p.Glu75Gln *hTWIST2* injection (Figure S3B) and all but one were up- or downregulated in the same fashion in both mutants (Figure S3C). The majority of expression changes of these target genes induced by overexpression of p.Glu75Lys and p.Glu75Gln were confirmed by analyzing the stable transgenic zebrafish embryos (Figure S3D). Gene ontology (GO) analyses revealed the greatest reduction in the expression of genes related to extracellular matrix (ECM), membrane components, and cytoskeleton (fibrils) (Figure 3E).

Discussion

We have shown that recurrent dominant mutations in the DNA binding domain of *TWIST2* are responsible for two ectodermal dysplasias associated with congenital malformations and dysmorphic facial features, i.e., AMS and BSS. All 10 AMS-affected and 11 of 12 BSS-affected individuals carried a mutation in the highly conserved p.Glu75 amino acid (either p.Glu75Lys, p.Glu75Gln, or p.Glu75Ala). Mutations in the basic domain of TWIST2 drastically altered the spectrum of DNA binding, reducing normal binding and increasing binding to off-target sites. The dominant nature of the mutations, then, could be explained by the abnormal 50% of TWIST2 homodimers and bHLH heterodimers that either reduced binding to the normal contingent of DNA binding sites or conferred a neomorphic function by binding to other sites. Based upon the multitude of DNA binding sites affected by AMS and BSS mutations, the phenotypic manifestations of both AMS and BSS probably result from transcriptional effects on more than a single gene. Our findings support the importance of the DNA binding domain of bHLH transcription factors: autosomal-dominant mutations in the DNA binding domain of *TWIST1* (GenBank: NM_000474.3; MIM: 601622), another member of the bHLH transcriptional regulators, have been associated with Saethre-Chotzen syndrome (MIM: 101400), which is characterized with craniosynostosis and limb abnormalities.[56,57]

Development appears to be exquisitely sensitive to the influence of TWIST2. Simple overexpression of the wild-type protein in zebrafish caused a mild developmental phenotype. In addition, although AMS and BSS result from missense mutations of the same amino acid, p.Glu75, the phenotypes depend on the substituting amino acid. A lysine at TWIST2 residue 75 results in AMS, whereas a glutamine or alanine yields BSS. This suggests that a single amino acid alteration, yielding two phenotypically distinct disorders, dictates specific groups of targeted developmental genes, some shared and some not shared between AMS and BSS (Figure S4B). Those genes might well encode proteins of the extracellular matrix, whose expression in zebrafish was downregulated by the mutations that cause AMS and BSS (Figure S3). In fact, the phenotypes of those zebrafish are reminiscent of *sly* and *bal* mutants,[58] which are loss-of-function alleles of gamma-1- and alpha-1-laminins, key components of the extracellular matrix. TWIST2 is recognized as a key regulator of mesenchymal cell fate during embryonic development and of epithelial-mesenchymal transition in human cancers;[59–63] therefore, TWIST2 mutations might alter the ECM by causing aberrant gene expression.

We conclude that recurrent dominant mutations in the DNA binding domain of *TWIST2* are responsible for AMS and BSS, ectodermal dysplasias with congenital malformations and dysmorphic facial features. All 10 AMS-affected and 11 of 12 BSS-affected individuals had an alteration in p.Glu75 of TWIST2. The zebrafish developmental anomalies arising from injection of mutant *TWIST2* RNA and ChIP studies suggest two possible mechanisms: a dominant-negative effect due to loss of binding to the normal contingent of TWIST2 DNA binding sites or a neomorphic mechanism due to binding of the mutant TWIST2 to extraneous promoter sites. Supporting a contribution by the first mechanism is the phenotypic overlap with Setleis syndrome (MIM: 227260), a less severe ectodermal dysplasia characterized by bitemporal lesions as well as eyelash and eyebrow defects,[64–68] that has been associated with homozygous loss-of-function mutations in *TWIST2*.

Supplemental Data

Acknowledgments

Web Resources

The URLs for data presented herein are as follows:

1000 Genomes Project (11_2010 data release), ftp://ftp-trace.ncbi.nih.gov/1000genomes/ftp/release/20100804/
CLINSEQ, http://www.genome.gov/20519355
dbSNP, http://www.ncbi.nlm.nih.gov/projects/SNP/
ExAC Browser (accessed 11, 2015), http://exac.broadinstitute.org/
FastQC, http://www.bioinformatics.babraham.ac.uk/projects/fastqc
Gene Ontology Consortium, http://geneontology.org/
Gorilla, http://cbl-gorilla.cs.technion.ac.il/
MACS, http://liulab.dfci.harvard.edu/MACS/00README.html
NHLBI Exome Sequencing Project (ESP) Exome Variant Server, http://evs.gs.washington.edu/EVS/

References

1. Cruz, A.A.V., Guimarães, F.C., Obeid, H.N., Ferraz, V.E.F., Noce, T.R., and Martinez, F.E. (1995). Congenital shortening of the anterior lamella of all eyelids: the so-called ablepharon macrostomia syndrome. Ophthal. Plast. Reconstr. Surg. *11*, 284–287.

2. Cruz, A.A., Souza, C.A., Ferraz, V.E., Monteiro, C.A., and Martins, F.A. (2000). Familial occurrence of ablepharon macrostomia syndrome: eyelid structure and surgical considerations. Arch. Ophthalmol. *118*, 428–430.

3. Amor, D.J., and Savarirayan, R. (2001). Intermediate form of ablepharon-macrostomia syndrome with CNS abnormalities. Am. J. Med. Genet. *103*, 252–254.

4. Barber, N., Say, B., Bell, R.F., and Merveille, O.C. (1982). Macrostomia, ectropion, atrophic skin, hypertrichosis and growth retardation. Syndr. Ident. *8*, 6–9.

5. Brancati, F., Mingarelli, R., Sarkozy, A., and Dallapiccola, B. (2004). Ablepharon-macrostomia syndrome in a 46-year-old woman. Am. J. Med. Genet. A. *127A*, 96–98.

6. Cavalcanti, D.P., Matejas, V., Luquetti, D., Mello, M.F., and Zenker, M. (2007). Fraser and Ablepharon macrostomia phenotypes: concurrence in one family and association with mutated FRAS1. Am. J. Med. Genet. A. *143A*, 241–247.

7. David, A., Gordeeff, A., Badoual, J., and Delaire, J. (1991). Macrostomia, ectropion, atrophic skin, hypertrichosis: another observation. Am. J. Med. Genet. *39*, 112–115.

8. Dinulos, M.B., and Pagon, R.A. (1999). Autosomal dominant inheritance of Barber-Say syndrome. Am. J. Med. Genet. *86*, 54–56.

9. Ferraz, V.E., Melo, D.G., Hansing, S.E., Cruz, A.A., and Pina-Neto, J.M. (2000). Ablepharon-macrostomia syndrome: first report of familial occurrence. Am. J. Med. Genet. *94*, 281–283.

10. Haensel, J., Kohlschmidt, N., Pitz, S., Keilmann, A., Zenker, M., Ullmann, R., Haaf, T., and Bartsch, O. (2009). Case report supporting that the Barber-Say and ablepharon macrostomia syndromes could represent one disorder. Am. J. Med. Genet. A. *149A*, 2236–2240.

11. Hornblass, A., and Reifler, D.M. (1985). Ablepharon macrostomia syndrome. Am. J. Ophthalmol. *99*, 552–556.

12. Jackson, I.T., Shaw, K.E., and del Pinal Matorras, F. (1988). A new feature of the ablepharon macrostomia syndrome: zygomatic arch absence. Br. J. Plast. Surg. *41*, 410–416.

13. Kallish, S., McDonald-McGinn, D.M., van Haelst, M.M., Bartlett, S.P., Katowitz, J.A., and Zackai, E.H. (2011). Ablepharon-Macrostomia syndrome–extension of the phenotype. Am. J. Med. Genet. A. *155A*, 3060–3062.

14. Martínez Santana, S., Pérez Alvarez, F., Frías, J.L., and Martínez-Frías, M.L. (1993). Hypertrichosis, atrophic skin, ectropion, and macrostomia (Barber-Say syndrome): report of a new case. Am. J. Med. Genet. *47*, 20–23.

15. Martins, F., Ortega, K.L., Hiraoka, C., Ricardo, P., and Magalhães, M. (2010). Oral and dental abnormalities in Barber-Say syndrome. Am. J. Med. Genet. A. *152A*, 2569–2573.

16. Mazzanti, L., Bergamaschi, R., Neri, I., Perri, A., Patrizi, A., Cacciari, E., and Forabosco, A. (1998). Barber-Say Syndrome: report of a new case. Am. J. Med. Genet. *78*, 188–191.

17. McCarthy, G.T., and West, C.M. (1977). Ablepheron macrostomia syndrome. Dev. Med. Child Neurol. *19*, 659–663.

18. Ng, J.D., and Rajguru, D.S. (2006). Oculoplastic approach to treating Barber-Say syndrome. Ophthal. Plast. Reconstr. Surg. *22*, 232–234.

19. Pellegrino, J.E., Schnur, R.E., Boghosian-Sell, L., Strathdee, G., Overhauser, J., Spinner, N.B., Stump, T., Grace, K., and Zackai, E.H. (1996). Ablepharon macrostomia syndrome with associated cutis laxa: possible localization to 18q. Hum. Genet. *97*, 532–536.

20. Price, N.J., Pugh, R.E., Farndon, P.A., and Willshaw, H.E. (1991). Ablepharon macrostomia syndrome. Br. J. Ophthalmol. *75*, 317–319.

21. Roche, N., Houtmeyers, P., Janssens, S., and Blondeel, P. (2010). Barber-Say syndrome in a father and daughter. Am. J. Med. Genet. A. *152A*, 2563–2568.

22. Rohena, L., Kuehn, D., Marchegiani, S., and Higginson, J.D. (2011). Evidence for autosomal dominant inheritance of able-pharon-macrostomia syndrome. Am. J. Med. Genet. A. *155A*, 850–854.

23. Sod, R., Izbizky, G., and Cohen-Salama, M. (1997). Macrostomia, hypertelorism, atrophic skin, severe hypertrichosis without ectropion: milder form of Barber-Say Syndrome. Am. J. Med. Genet. *73*, 366–367.

24. Stevens, C.A., and Sargent, L.A. (2002). Ablepharon-macrostomia syndrome. Am. J. Med. Genet. *107*, 30–37.

25. Tenea, D., and Jacyk, W.K. (2006). What syndrome is this? Barber-Say syndrome. Pediatr. Dermatol. *23*, 183–184.

26. Cortes, F.M., Troncoso, L.A., Alliende, A.R., and Curotto, B.L. (2000). Barber-Say syndrome: further delineation of the clinical spectrum. Genet. Mol. Biol. *23*, 265–267.

27. Allanson, J.E., Cunniff, C., Hoyme, H.E., McGaughran, J., Muenke, M., and Neri, G. (2009). Elements of morphology: standard terminology for the head and face. Am. J. Med. Genet. A. *149A*, 6–28.

28. Biesecker, L.G., Aase, J.M., Clericuzio, C., Gurrieri, F., Temple, I.K., and Toriello, H. (2009). Elements of morphology: standard terminology for the hands and feet. Am. J. Med. Genet. A. *149A*, 93–127.

29. Carey, J.C., Cohen, M.M., Jr., Curry, C.J., Devriendt, K., Holmes, L.B., and Verloes, A. (2009). Elements of morphology: standard terminology for the lips, mouth, and oral region. Am. J. Med. Genet. A. *149A*, 77–92.

30. Hall, B.D., Graham, J.M., Jr., Cassidy, S.B., and Opitz, J.M. (2009). Elements of morphology: standard terminology for the periorbital region. Am. J. Med. Genet. A. *149A*, 29–39.

31. Hennekam, R.C., Allanson, J.E., Biesecker, L.G., Carey, J.C., Opitz, J.M., and Vilain, E. (2013). Elements of morphology: standard terminology for the external genitalia. Am. J. Med. Genet. A. *161A*, 1238–1263.

32. Hennekam, R.C., Cormier-Daire, V., Hall, J.G., Méhes, K., Patton, M., and Stevenson, R.E. (2009). Elements of morphology: standard terminology for the nose and philtrum. Am. J. Med. Genet. A. *149A*, 61–76.

33. Hunter, A., Frias, J.L., Gillessen-Kaesbach, G., Hughes, H., Jones, K.L., and Wilson, L. (2009). Elements of morphology: standard terminology for the ear. Am. J. Med. Genet. A. *149A*, 40–60.

34. Klinger, G., and Merlob, P. (2009). Elements of morphology: standard terminology for the ear–additional features. Am. J. Med. Genet. A. *149A*, 1606, author reply 1607.

35. Li, L., Cserjesi, P., and Olson, E.N. (1995). Dermo-1: a novel twist-related bHLH protein expressed in the developing dermis. Dev. Biol. *172*, 280–292.

36. Barnes, R.M., and Firulli, A.B. (2009). A twist of insight - the role of Twist-family bHLH factors in development. Int. J. Dev. Biol. *53*, 909–924.

37. Gong, X.Q., and Li, L. (2002). Dermo-1, a multifunctional basic helix-loop-helix protein, represses MyoD transactivation via the HLH domain, MEF2 interaction, and chromatin deacetylation. J. Biol. Chem. *277*, 12310–12317.

38. Sosic, D., and Olson, E.N. (2003). A new twist on twist–modulation of the NF-kappa B pathway. Cell Cycle *2*, 76–78.

39. Šošić, D., Richardson, J.A., Yu, K., Ornitz, D.M., and Olson, E.N. (2003). Twist regulates cytokine gene expression through a negative feedback loop that represses NF-kappaB activity. Cell *112*, 169–180.

40. Isenmann, S., Arthur, A., Zannettino, A.C., Turner, J.L., Shi, S., Glackin, C.A., and Gronthos, S. (2009). TWIST family of basic helix-loop-helix transcription factors mediate human mesenchymal stem cell growth and commitment. Stem Cells *27*, 2457–2468.

41. Lee, M.S., Lowe, G., Flanagan, S., Kuchler, K., and Glackin, C.A. (2000). Human Dermo-1 has attributes similar to twist in early bone development. Bone *27*, 591–602.

42. Cullinane, A.R., Vilboux, T., O'Brien, K., Curry, J.A., Maynard, D.M., Carlson-Donohoe, H., Ciccone, C., Markello, T.C., Gunay-Aygun, M., Huizing, M., and Gahl, W.A.; NISC Comparative Sequencing Program (2011). Homozygosity mapping and whole-exome sequencing to detect SLC45A2 and G6PC3 mutations in a single patient with oculocutaneous albinism and neutropenia. J. Invest. Dermatol. *131*, 2017–2025.

43. Markello, T.C., Han, T., Carlson-Donohoe, H., Ahaghotu, C., Harper, U., Jones, M., Chandrasekharappa, S., Anikster, Y., Adams, D.R., Gahl, W.A., and Boerkoel, C.F.; NISC Comparative Sequencing Program (2012). Recombination mapping using Boolean logic and high-density SNP genotyping for exome sequence filtering. Mol. Genet. Metab. *105*, 382–389.

44. Gahl, W.A., Markello, T.C., Toro, C., Fajardo, K.F., Sincan, M., Gill, F., Carlson-Donohoe, H., Gropman, A., Pierson, T.M., Golas, G., et al. (2012). The National Institutes of Health Undiagnosed Diseases Program: insights into rare diseases. Genet. Med. *14*, 51–59.

45. Gahl, W.A., and Tifft, C.J. (2011). The NIH Undiagnosed Diseases Program: lessons learned. JAMA *305*, 1904–1905.

46. Li, H., and Durbin, R. (2009). Fast and accurate short read alignment with Burrows-Wheeler transform. Bioinformatics *25*, 1754–1760.

47. Zhang, Y., Liu, T., Meyer, C.A., Eeckhoute, J., Johnson, D.S., Bernstein, B.E., Nusbaum, C., Myers, R.M., Brown, M., Li, W., and Liu, X.S. (2008). Model-based analysis of ChIP-Seq (MACS). Genome Biol. *9*, R137.

48. Quinlan, A.R., and Hall, I.M. (2010). BEDTools: a flexible suite of utilities for comparing genomic features. Bioinformatics *26*, 841–842.

49. Shin, H., Liu, T., Manrai, A.K., and Liu, X.S. (2009). CEAS: cis-regulatory element annotation system. Bioinformatics *25*, 2605–2606.

50. Machanick, P., and Bailey, T.L. (2011). MEME-ChIP: motif analysis of large DNA datasets. Bioinformatics *27*, 1696–1697.

51. Westerfield, M. (2000). The Zebrafish Book. A Guide for the Laboratory Use of Zebrafish (*Danio rerio*) (Eugene: University of Oregon Press).

52. Dobin, A., Davis, C.A., Schlesinger, F., Drenkow, J., Zaleski, C., Jha, S., Batut, P., Chaisson, M., and Gingeras, T.R. (2013). STAR: ultrafast universal RNA-seq aligner. Bioinformatics *29*, 15–21.

53. Anders, S., and Huber, W. (2010). Differential expression analysis for sequence count data. Genome Biol. *11*, R106.

54. Eden, E., Navon, R., Steinfeld, I., Lipson, D., and Yakhini, Z. (2009). GOrilla: a tool for discovery and visualization of enriched GO terms in ranked gene lists. BMC Bioinformatics *10*, 48.

55. Eden, E., Lipson, D., Yogev, S., and Yakhini, Z. (2007). Discovering motifs in ranked lists of DNA sequences. PLoS Comput. Biol. *3*, e39.

56. el Ghouzzi, V., Le Merrer, M., Perrin-Schmitt, F., Lajeunie, E., Benit, P., Renier, D., Bourgeois, P., Bolcato-Bellemin, A.L.,

Munnich, A., and Bonaventure, J. (1997). Mutations of the TWIST gene in the Saethre-Chotzen syndrome. Nat. Genet. *15*, 42–46.

57. Howard, T.D., Paznekas, W.A., Green, E.D., Chiang, L.C., Ma, N., Ortiz de Luna, R.I., Garcia Delgado, C., Gonzalez-Ramos, M., Kline, A.D., and Jabs, E.W. (1997). Mutations in TWIST, a basic helix-loop-helix transcription factor, in Saethre-Chotzen syndrome. Nat. Genet. *15*, 36–41.

58. Stemple, D.L., Solnica-Krezel, L., Zwartkruis, F., Neuhauss, S.C., Schier, A.F., Malicki, J., Stainier, D.Y., Abdelilah, S., Rangini, Z., Mountcastle-Shah, E., and Driever, W. (1996). Mutations affecting development of the notochord in zebrafish. Development *123*, 117–128.

59. Floc'h, N., Kolodziejski, J., Akkari, L., Simonin, Y., Ansieau, S., Puisieux, A., Hibner, U., and Lassus, P. (2013). Modulation of oxidative stress by twist oncoproteins. PLoS ONE *8*, e72490.

60. Fu, J., Qin, L., He, T., Qin, J., Hong, J., Wong, J., Liao, L., and Xu, J. (2011). The TWIST/Mi2/NuRD protein complex and its essential role in cancer metastasis. Cell Res. *21*, 275–289.

61. Gasparotto, D., Polesel, J., Marzotto, A., Colladel, R., Piccinin, S., Modena, P., Grizzo, A., Sulfaro, S., Serraino, D., Barzan, L., et al. (2011). Overexpression of TWIST2 correlates with poor prognosis in head and neck squamous cell carcinomas. Oncotarget *2*, 1165–1175.

62. Wang, T., Li, Y., Wang, W., Tuerhanjiang, A., Wu, Z., Yang, R., Yuan, M., Ma, D., Wang, W., and Wang, S. (2014). Twist2, the key Twist isoform related to prognosis, promotes invasion of cervical cancer by inducing epithelial-mesenchymal transition and blocking senescence. Hum. Pathol. *45*, 1839–1846.

63. Teng, Y., and Li, X. (2014). The roles of HLH transcription factors in epithelial mesenchymal transition and multiple molecular mechanisms. Clin. Exp. Metastasis *31*, 367–377.

64. Cervantes-Barragán, D.E., Villarroel, C.E., Medrano-Hernández, A., Durán-McKinster, C., Bosch-Canto, V., Del-Castillo, V., Nazarenko, I., Yang, A., and Desnick, R.J. (2011). Setleis syndrome in Mexican-Nahua sibs due to a homozygous TWIST2 frameshift mutation and partial expression in heterozygotes: review of the focal facial dermal dysplasias and subtype reclassification. J. Med. Genet. *48*, 716–720.

65. Franco, H.L., Casasnovas, J.J., Leon, R.G., Friesel, R., Ge, Y., Desnick, R.J., and Cadilla, C.L. (2011). Nonsense mutations of the bHLH transcription factor TWIST2 found in Setleis Syndrome patients cause dysregulation of periostin. Int. J. Biochem. Cell Biol. *43*, 1523–1531.

66. Rosti, R.O., Uyguner, Z.O., Nazarenko, I., Bekerecioglu, M., Cadilla, C.L., Ozgur, H., Lee, B.H., Aggarwal, A.K., Pehlivan, S., and Desnick, R.J. (2014). Setleis syndrome: clinical, molecular and structural studies of the first TWIST2 missense mutation. Clin. Genet. Published online December 11, 2014. http://dx.doi.org/10.1111/cge.12539.

67. Tukel, T., Šošić, D., Al-Gazali, L.I., Erazo, M., Casasnovas, J., Franco, H.L., Richardson, J.A., Olson, E.N., Cadilla, C.L., and Desnick, R.J. (2010). Homozygous nonsense mutations in TWIST2 cause Setleis syndrome. Am. J. Hum. Genet. *87*, 289–296.

68. Girisha, K.M., Bidchol, A.M., Sarpangala, M.K., and Satyamoorthy, K. (2014). A novel frameshift mutation in TWIST2 gene causing Setleis syndrome. Indian J. Pediatr. *81*, 302–304.
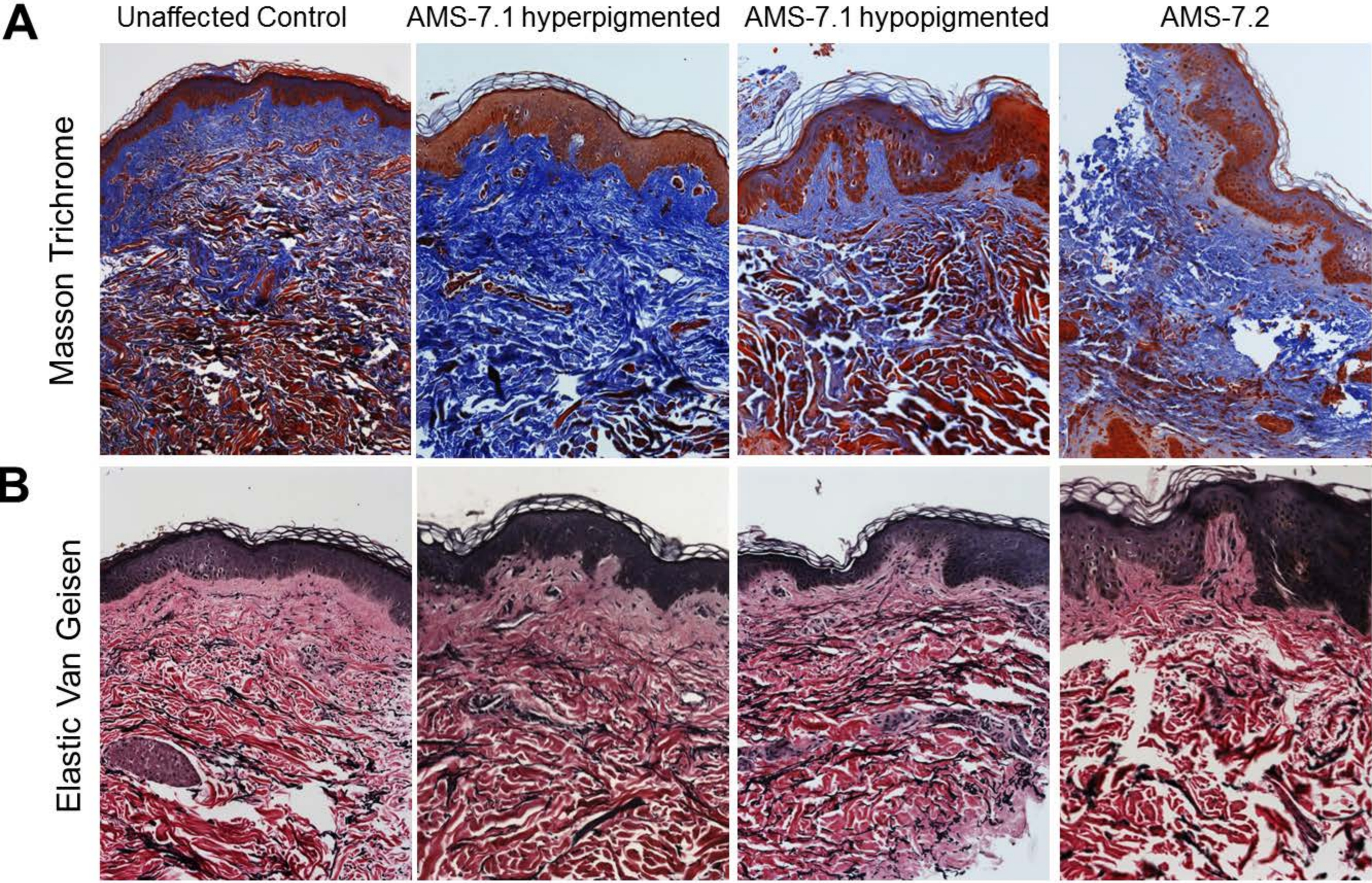
Recurrent Mutations in the Basic Domain

of *TWIST2* Cause Ablepharon Macrostomia

and Barber-Say Syndromes

Shannon Marchegiani, Taylor Davis, Federico Tessadori, Gijs van Haaften, Francesco Brancati, Alexander Hoischen, Haigen Huang, Elise Valkanas, Barbara Pusey, Denny Schanze, Hanka Venselaar, Anneke T. Vulto-van Silfhout, Lynne A. Wolfe, Cynthia J. Tifft, Patricia M. Zerfas, Giovanna Zambruno, Ariana Kariminejad, Farahnaz Sabbagh-Kermani, Janice Lee, Maria G. Tsokos, Chyi-Chia R. Lee, Victor Ferraz, Eduarda Morgana da Silva, Cathy A. Stevens, Nathalie Roche, Oliver Bartsch, Peter Farndon, Eva Bermejo-Sanchez, Brian P. Brooks, Valerie Maduro, Bruno Dallapiccola, Feliciano J. Ramos, Hon-Yin Brian Chung, Cédric Le Caignec, Fabiana Martins, Witold K. Jacyk, Laura Mazzanti, Han G. Brunner, Jeroen Bakkers, Shuo Lin, May Christine V. Malicdan, Cornelius F. Boerkoel, William A. Gahl, Bert B.A. de Vries, Mieke M. van Haelst, Martin Zenker, and Thomas C. Markello

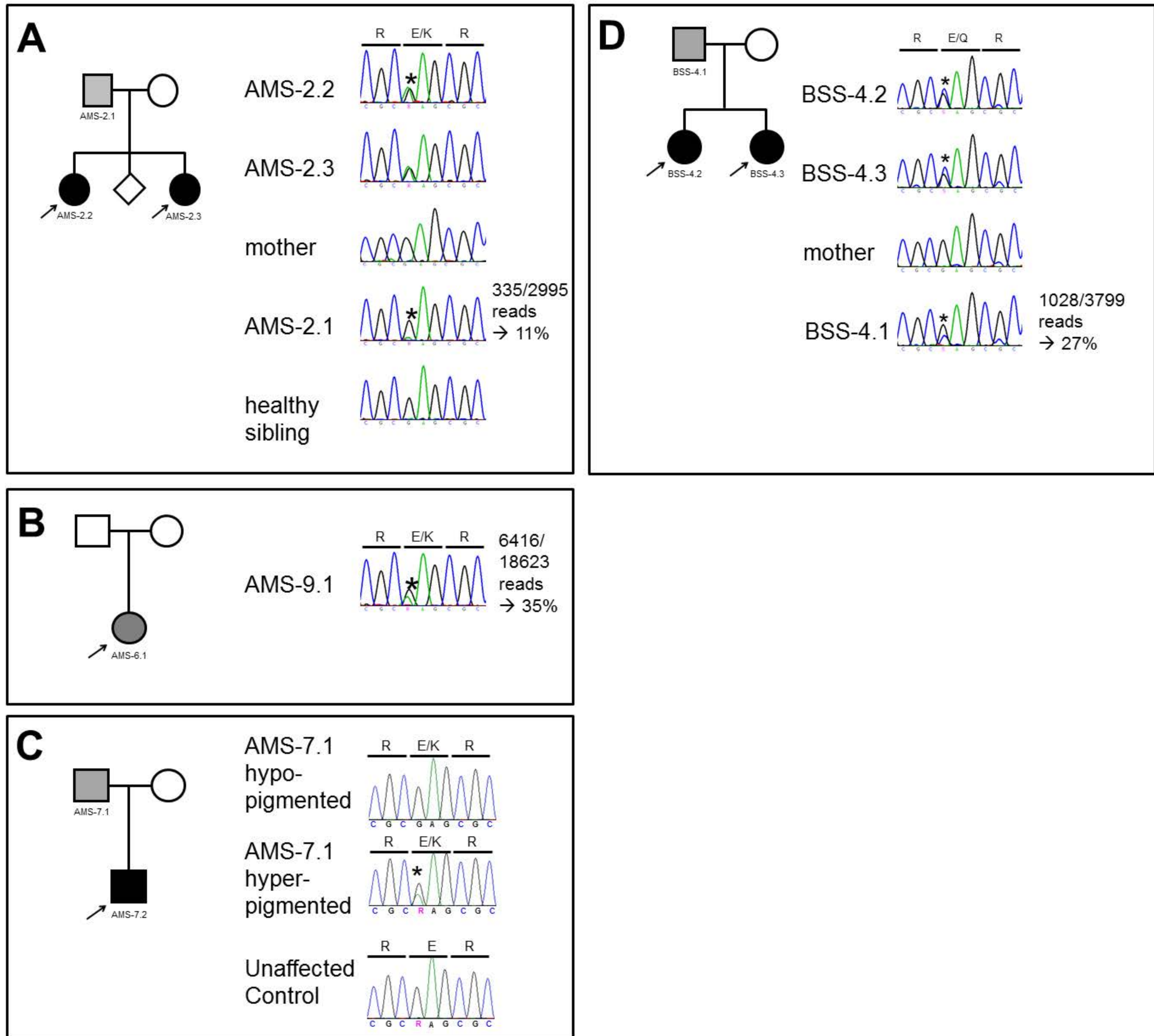# Supplementary Figures
Figure S1

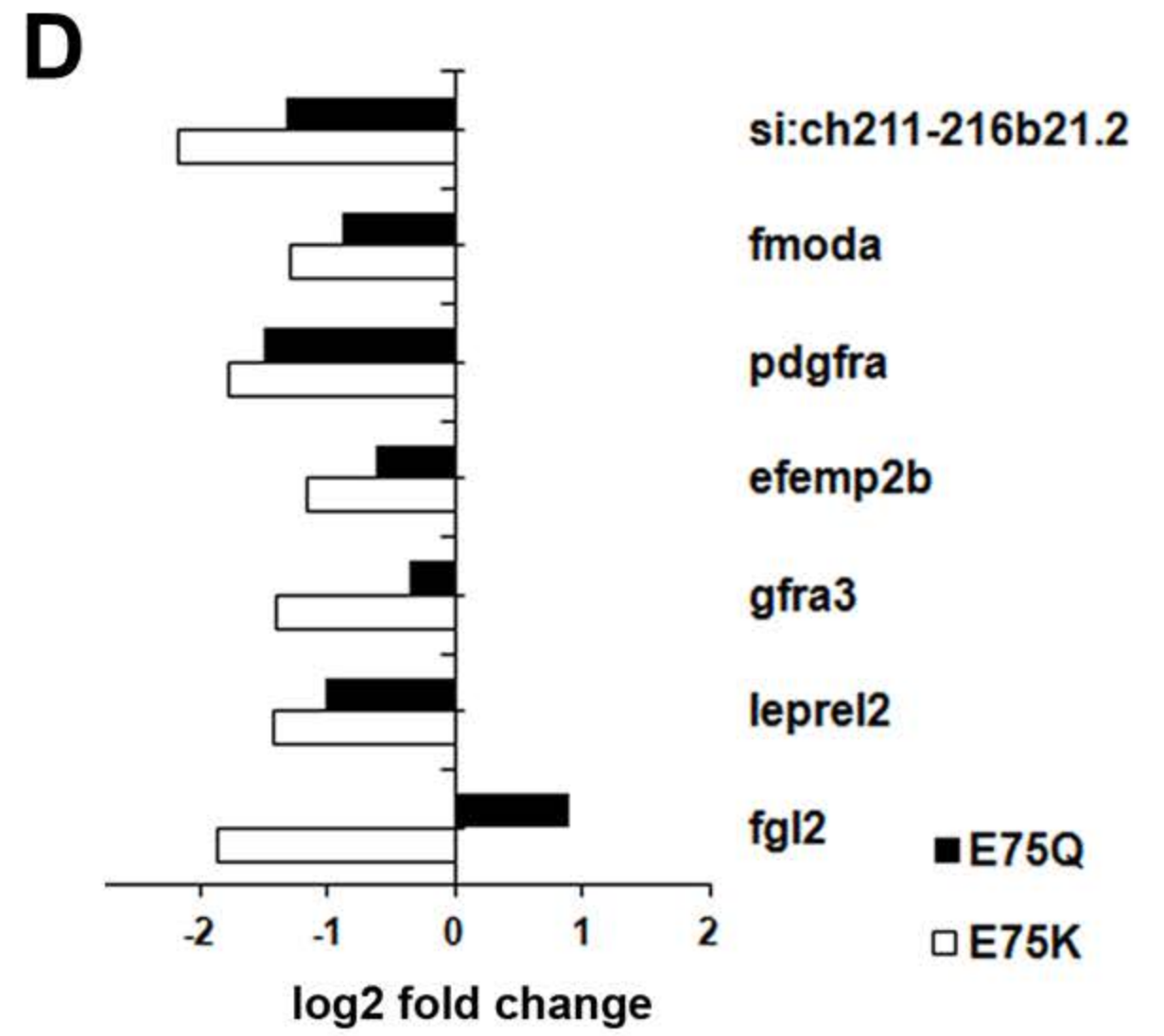**A** | Unaffected Control | AMS-7.1 hyperpigmented | AMS-7.1 hypopigmented | AMS-7.2 (Masson Trichrome)

B | Unaffected Control | AMS-7.1 hyperpigmented | AMS-7.1 hypopigmented | AMS-7.2 (Elastic Van Geisen)

Figures

Figure S2

Figure S3

A

hTwist2/cre heated

E75Q/cre heated

E75K/cre heated

B

E75K (AMS)   E75Q (BSS)

111   28   23

C

CT956064.3
efemp2b
leprel2
BX296557.7
crabp2b
slc38a2
fgl2
myclb
emilin2a
hmcn2
C8H1orf106
fam107b
hk1
BX548021.2
si:dkey-253d23.4
exoc3l1
ntd5
colec12
si:ch211-216b21.2
slc38a5a
hhip
syneb
si:ch211-267e7.3
fbln5
rnf144aa
fmoda
pdgfra
gfra3

□ E75K
■ E75Q

log2 fold change

D

si:ch211-216b21.2
fmoda
pdgfra
efemp2b
gfra3
leprel2
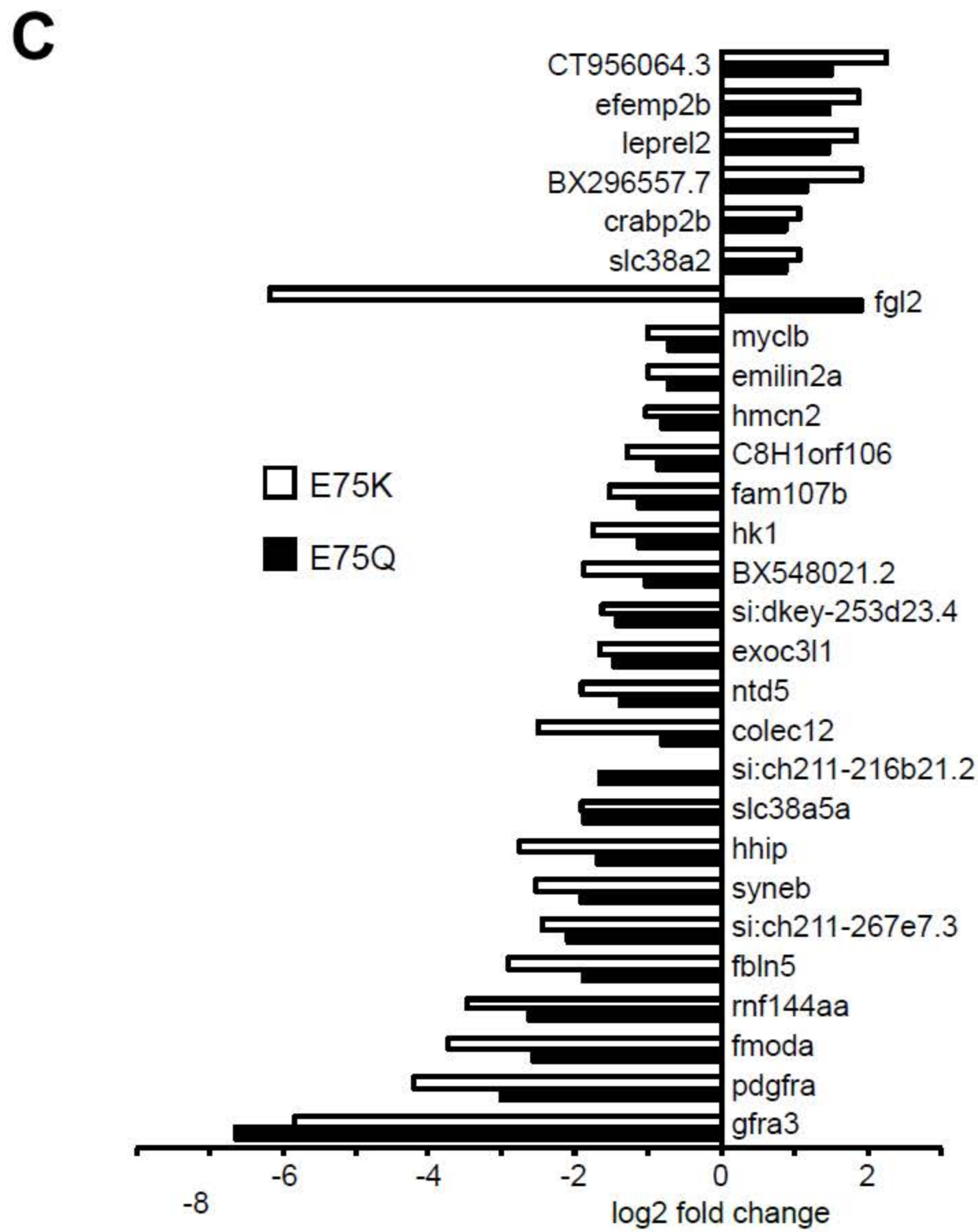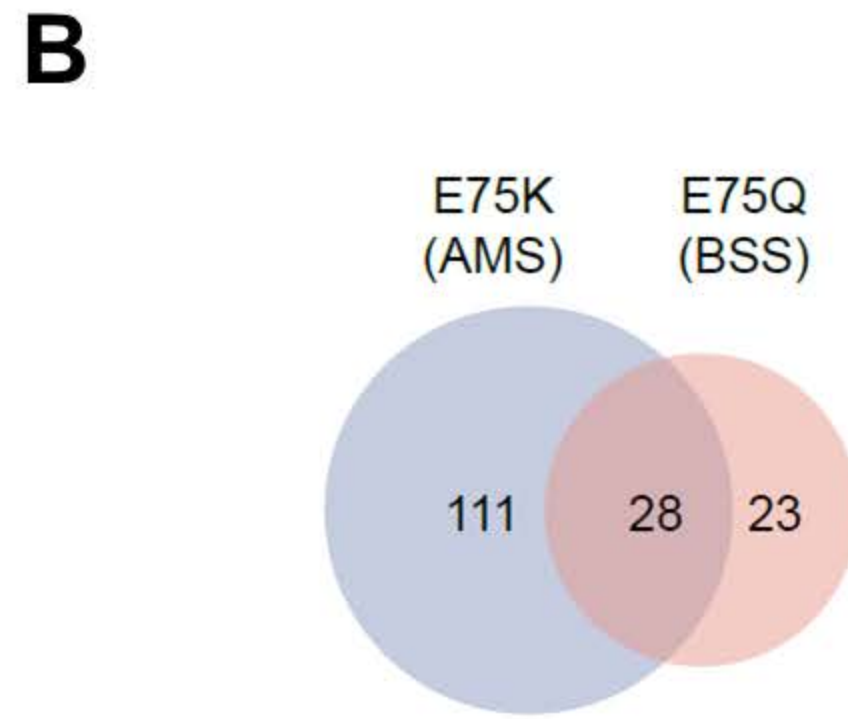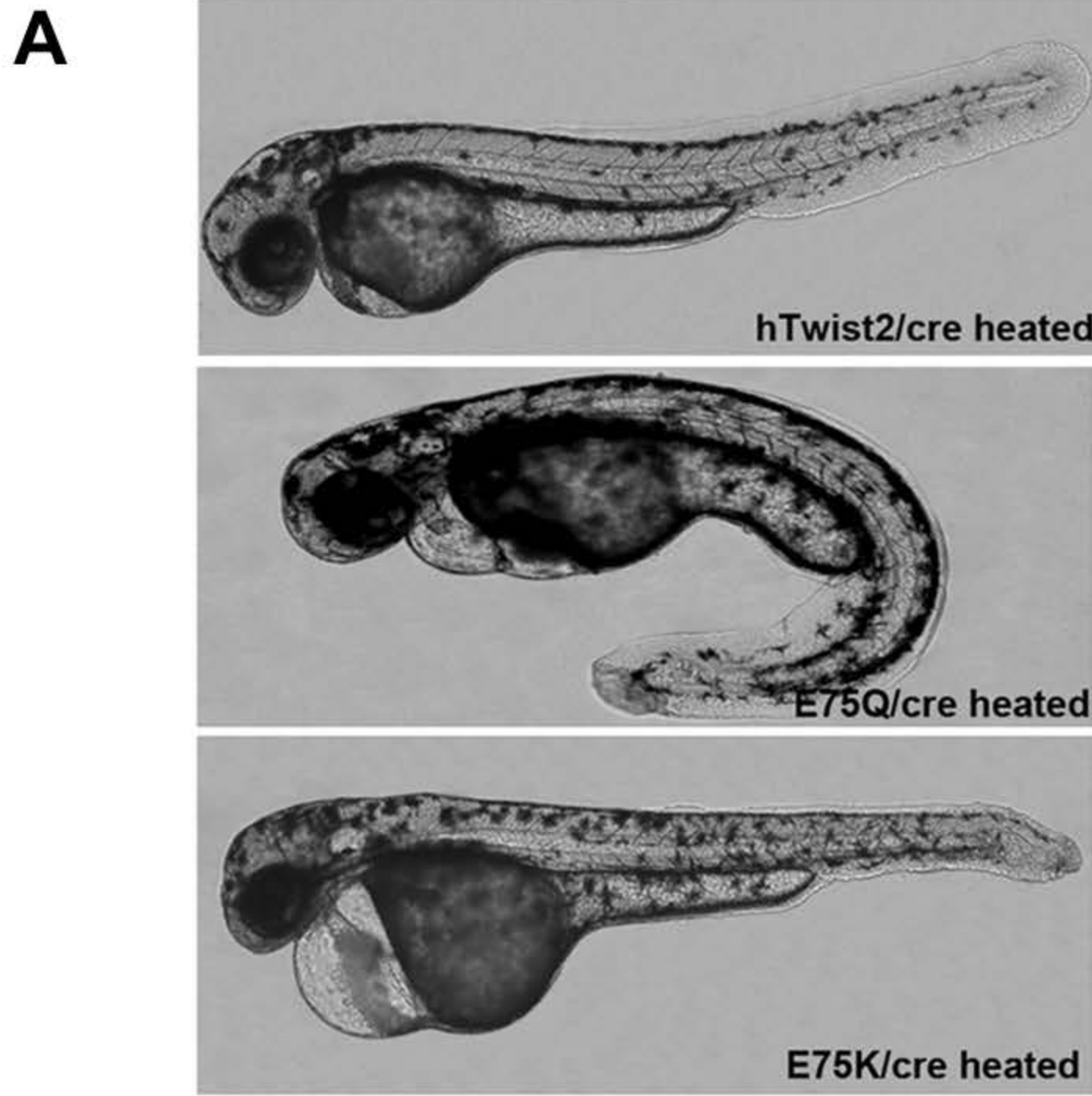fgl2

■ E75Q
□ E75K

log2 fold change

Supplemental Data

Supplemental Figure Legends

Figure S1: Skin biopsies in AMS family 7.

Photomicrographs of full thickness Hematoxylin and Eosin staining of paraffin embedded skin from an unaffected control, AMS-7.1 hyperpigmented (affected) and hypopigmented (unaffected) areas, and AMS-7.2. The tissue was stained with Masson trichrome to demonstrate collagen fibers (blue) or Elastic Tissue Fibers – Verhoeff's Van Gieson (EVG) stains to show elastic fibers (black), which are prominent in the reticular dermis.

Figure S2: Chromatograms showing mosaicism of AMS and BSS families

a, **b**, and **d** were confirmed by next generation sequencing on a Roche GS Junior. **c** results were confirmed by sequencing DNA extracted from dermal fibroblasts derived from hypopigmented (unaffected) and hyperpigmented (affected) skin. Asterisk highlights the mutation.

Figure S3: Zebrafish

a. Defective morphology was observed in all transgenic embryos induced by *Cre* at 2 dpf but mutant p.Glu75Lys (E75K) and p.Glu75Gln (E75Q) embryos displayed stronger phenotype compared to the wild type TWIST2.

b. Venn diagram analysis of differentially-expressed genes in the *hTWIST2* p.Glu75Lys (E75K) and p.Glu75Gln (E75Q) overexpression libraries.

c. Cut-off for selection of genes: padj<0.05. The 28 overlapping genes are listed with the level of up-regulation or down-regulation relative to wild-type *hTWIST2*-overexpressing samples. Data were collected from 3 biologically and technically independent experiments.

d. Seven target genes were chosen from RNA-Seq results for qPCR validation using transgenic lines. Compared to the wild type, p.Glu75Lys (E75K) appeared to be more potent than p.Glu75Gln (E75Q) in suppressing targeted genes. It is worth noting that *fgl2*

was enhanced in p.Glu75Gln (E75Q) but repressed by p.Glu75Lys (E75K), suggesting some difference between the two mutations in inducing the disease.

Supplemental Table

TABLE S1. Primers used for sequencing cloning, and zebrafish experiments

Primer Name	Primer Sequence
TWIST2_FLAG_HA_GC_F1	CACCATGGACTACAAGGACGACGATGACAAAGTCAAG TCTACCCATACGATGTTCCAGATTACGCTGCTGCTATG GAGGAGGGCTCCAGC
FLAG_HA_mutagenesisfix_F	GATGACAAAGTCAAGCTCTACCCATACGATG
FLAG_HA_mutagenesisfix_R	CATCGTATGGGTAGAGCTTGACTTTGTCATC
TWIST2GATERSTOP	CTAGTGGGAGGCGGACAT
TWIST2SangerSequencingF	CAGAGCCTTTCCAGCAACTC
TWIST2SangerSequencingR	AGCGTGGGGATGATCTTG
TWIST2_E75Q_mutF	GCGCTGGCGCTGGCGCACGTTGG
TWIST2_E75Q_mutR	CCAACGTGCGCCAGCGCCAGCGC
TWIST2_E75A_mutF	TGCGCTGGCGCGCGCGCACGTTG
TWIST2_E75A_mutR	CAACGTGCGCGCGCGCCAGCGCA
TWIST2_R77_Q78dup_mutF	CGTGCGCGAGCGCCAGCGCCAGCGCACCCAGTCGCTC
TWIST2_R77_Q78dup_mutR	GAGCGACTGGGTGCGCTGGCGCTGGCGCTCGCGCACG
TWIST2_E75K_mutF	CAACGTGCGCAAGCGCCAGCG
TWIST2_E75K_mutR	CGCTGGCGCTTGCGCACGTTG
fg12_F	TGGTCAATAAAATCAGCAGCAC
fg12_R	CCTCTGAGTCTTCCAGCTCAAT
efemp2_F	GGTGGTTACCTGTGTCTTCCTC
efemp2_R	CCTGGTTCACACTCACAAGAGA
leprel2_F	CAGGCAGTGGATTATCATCAGA
leprel2_R	AGACACTTCGACTCATGCAGAA
gfra3_F	CTGTTTAGAGGCTCTCCAGGAA
gfra3_R	AAACTATGGAGGCCAGTTTTGA
pdgfra_F	GACGTTCCTGAGGTTGTAGACC
pdgfra_R	AATGAGCTCTCGTGAACTGTGA
fmoda_F	GGCCAATCAGATCAAAGAGTTC
fmoda_R	GATAAAACAAATTGGCTGCACA
si:ch211-216b21.2_F	CAGATAAGCGCATGTTTCTGTC
si:ch211-216b21.2_R	GGAGCTTCTCGAGTGACAAAGT

Supplemental Methods

Histology

Skin biopsy specimens were fixed in 10% neutral buffered formalin, routinely processed, and embedded in paraffin. After deparaffinization of 4-5 μm sections, the slides were subjected to a series of rehydration steps. Slides were stained with Masson Trichrome and Elastic Tissue Fibers - Verhoeff's Van Gieson (EVG) stains following standard protocols.

Zebrafish

Stable transgenic zebrafish lines expressing human wild type and mutant human *TWIST2* (p.Glu75Lys and p.Glus75Gln) under the control of a Cre-loxP inducible system were generated using a Tol2 based transgenic technology. Wild type or mutant *TWIST2* cDNA were placed downstream of zebrafish β-actin promoter, in which mCherry-STOP signal with two loxP elements at the both ends was placed between *TWIST2* gene sequence and β-actin promoter. Upon introduction of Cre, the mCherry-STOP cassette will be removed, functioning as an inducible element. Phenotypes of transgenic embryos were analyzed upon induction of Cre by heat at 38.5˚C for 30 minutes at 24hpf using heat-shock hs-Cre (+/-) and Twist2 (+/-) double transgenic zebrafish embryos. For qPCR, 60 transgenic embryos were heated at 38.5˚C for 30 minutes at 80% epiboly stage and then collected for RNA preparation in Trizol three hours later.